Supporting Online Material

Materials and Methods

Animals

Experiments were carried out using 5 - 8 week old C57BL/6J, mT1R2$^{-/-}$ (*S1*) or mT2R5$^{-/-}$ (*S2*) mice; all animal care was in accordance with institutional guidelines. Cortical imaging data were obtained in animals anesthetized with 1.6 mg / g urethane, delivered in two intra-peritoneal injections separated by 30 min. For thalamic recordings and AAV viral injections, animals were anesthetized with ketamine / xylazine (at a ratio of 100 / 10 mg per kg). Supplemental local anesthesia was provided by injection of 2% lidocaine prior to skin incisions; core-body temperature of anesthetized animals was maintained at 37 ˚C using a feedback controlled heating pad.

Recordings and viral tracing of taste-responsive neurons in the thalamus

A small hole was drilled into the skull of 5 - 8 week old C57BL/6J animals at ~0.65 mm from the midline and 2.0 mm caudal to the bregma. A tungsten recording electrode was introduced through this opening and advanced approximately 4.2 mm from the pia into the taste responsive ventromedial posteromedial nucleus of the thalamus [VPM; (*S3*)]. Lingual stimulation and extracellular recordings were as described previously for chorda tympani nerve recordings (*S1, S4*). Signal was amplified, bandpass filtered at 300 - 10, 000 Hz, and digitized. Spikes were identified using a custom Matlab routine that seeks signals that are equal or greater than 4 standard deviations from the baseline. 200 nl of AAV2/Hu11-GFP (*S5*) was pressure injected into the taste-responsive region of the VPM using a nanoliter injector. Two weeks after viral infection, the insular cortex was exposed and DiI was applied to mark the intersection of the middle cerebral artery (MCA) and rhinal veins (RV). The brain was fixed in 4% paraformaldehyde in phosphate buffered saline and sectioned. Sections (100 μm) were counterstained with TO-PRO-3 (1:1000) to highlight cortical layers and imaged for GFP, DiI and TO-PRO-3 fluorescence using confocal microscopy.

Accessing the insular cortex for imaging and recordings

Animals were tracheotomized under 1.6 mg / g urethane anesthesia, and both sides of the hypoglossal nerve were severed to immobilize the tongue. Additional anesthesia was provided using 1-2% isoflurane ventilated through the tracheotomy incision; the mouse's head was secured in a custom-made holder using dental acrylic to eliminate the risk of damaging the taste responsive chorda tympani nerve during surgery. To gain access to the insular cortex, an incision was made to expose the masseter muscle, and the mandible was then retracted to reveal the ventral-lateral surface of the skull; this allowed clear visualization of the lateral olfactory tract, the MCA and RV; as vascular landmarks varied slightly from animal to animal, many imaging fields were explored near the location of the expected hot spots. A custom-made chamber was cemented to the skull (to create a watertight compartment), and a small 1 x 1 mm craniotomy, approximately 2 mm dorsal to the lateral olfactory tract and either anterior or posterior to the MCA (see Fig. 1), was drilled over the insular cortex. After removal of the skull, the chamber was filled with warmed (37 ˚C) artificial cerebrospinal fluid (ACSF): 125 mM NaCl, 5 mM KCl, 10 mM glucose, 10 mM HEPES pH 7.4, 2 mM $CaCl_2$, and 2 mM $MgCl_2$. While hot spots were identified by following vascular landmarks, it should be noted that the relative positions of cortical arteries and veins often varies slightly between animals leading to small variations in the relative location of the hot spots after reconstruction (see for example Fig 2f and 4a). The bitter cortical field was located ~1 mm dorsal to the rhinal veins and ~1 mm posterior to the MCA; the sweet hotspot was approximately 2.5 mm rostro-dorsal to the bitter field; the umami hot spot was approximately 1 mm ventral to the sweet cortical field and the NaCl cortical field was approximately 1 mm from both the sweet and umami hot spots.

For single unit recording, a tungsten electrode (resistance 2.0-4.0 MΩ) was used to isolate individual gustatory neurons in the insular cortex. The electrode was advanced through the dura and into the brain with an electronically controlled micropositioner. Signals were amplified, bandpass filtered at 600-6000 Hz, and digitized with a Neuralynx data acquisition system. A neuron was considered a responder (i.e. to sweet, bitter, sour, umami or salty stimuli) if the increase in spike frequency was statistically significant above the pre-stimulation rate (one-way ANOVA $P < 0.05$); spike activity during the 5 sec window of tastant application was averaged for each trial ($n \geq 6$) and for each of the 5 taste qualities.

Dye Injections

Neurons in layer 2-3 of the insular cortex were bulk-loaded with the calcium-sensitive dye Oregon Green 488 BAPTA-1 AM (OGB-AM) under two-photon microscopy as described previously (*S6-S8*). We used glass pipettes with 5 μm tips to inject a solution containing 0.5 mM OGB-AM, 25 μM sulforhodamine 101, 4 % dimethylsulfoxide and 0.8 % (w/v) Pluronic F-127 in Ca^{2+}/Mg^{2+} free ACSF; the dye solution was maintained at 0 ˚C. Neurons were bulk-loaded over 5 min. by applying 100 - 200 ms pulses of 5 - 10 psi to the pipette to pressure eject dye at several sites approx. 300 μm apart from each other, and 200 - 250 μm below the surface of the insula. This procedure loaded hundreds of cells in an area with a diameter of about 600 μm (see Fig. 1d). After dye injection, the craniotomy was covered with 1.5% agarose in ACSF and sealed using dental acrylic with a No. 0 glass coverslip pre-cut to fit inside the custom chamber; this type of cranial window significantly decreased brain movement (*S7*).

Functional Imaging

Two-photon imaging was carried out using a two-photon microscope with a 40x water immersion objective (IR, N.A. = 0.8). This provided a 350 x 350 μm field of view that was scanned at 2-4 Hz and recorded as a series of 256 x 256 pixel images; we generally used 2 Hz as a compromise between high-quality images and full field imaging. No differences in results or conclusions were seen when imaging at 4 Hz. The excitation wavelength was 810 nm and fluorescence emission was filtered with a 580 dcxr dichroic and hq525/70 m-2p bandpass filter. Taste stimuli were delivered rapidly (> 2 ml / min.) to the entire tongue and oral cavity using a pressure-controlled perfusion system. For all experiments, a 30 s pre-stimulus application of artificial saliva (AS) preceded 10 s exposure to the test tastants and was followed by a 30 s AS wash; inter-trial window was 2 min. Unlike studies in the olfactory, visual, auditory or somatosensory system where the stimuli can be delivered and removed within milliseconds, and dozens of trials readily tested, the need to deliver significant amount of fluid to the tongue, and to thoroughly remove and wash the oral cavity between trials necessitates long trial times, thus limiting the total number of trials that can be tested in any one experiment. In general, one out of 4 animals could be successfully imaged (failures likely due to problems with damage to brain during surgery, OGB loading the correct cortical fields, difficulties with anesthesia, proper triangulation of vascular landmarks, etc); 4 - 8 trials (typically consisting of a series of 7

different tastants and AS in each trial) were imaged in each cortical field of view. Tastants used in our study were the highest available grade from Sigma and were dissolved in AS (*S1, S4*). Tastants were: 1 mM cycloheximide; 10 mM quinine; 10 mM denatonium benzoate; 30 mM acesulfameK; 300 mM sucrose; 100 mM mono potassium L-glutamate (MPG) + 1 mM inosine monophosphate (IMP); 100 mM L-serine + 1 mM IMP; 100 mM D-tryptophan + 1 mM IMP; 100 mM NaCl (low salt); 100 mM NaCl + 10 μM amiloride; 100 mM KCl; 100 mM MgCl2; 10mM citric acid.

After functional recording, the blood vessel patterns both on the surface of the cortical field of view and in adjacent areas, were imaged as reference points for spatial reconstructions. We also regularly recorded the blood vessel pattern over the entire craniotomy to assist in generating response maps from multiple imaging sites.

Image Analysis

The imaging data were analyzed using custom software written in Matlab. Lateral motion artifacts were corrected using the Image Stabilizer plugin in ImageJ. We then averaged the raw images across the entire t-series (i.e. 140 frames for 70s at a 2 Hz sampling rate) to generate a template used to delineate the outline of the neurons in the imaging field of view. Cell bodies were semi-automatically detected using a fast normalized cross-correlation routine. Briefly, the averaged images were cross-correlated against a kernel with a size approximating that of an average cell; this image map was thresholded to generate a binary mask that demarcated the cell bodies; about 200 neurons were found in a typical field of view (*S9*). Cellular fluorescence intensity (F_t) was calculated for the individual neurons at each time-point by averaging the intensity of pixels falling within the cell boundaries. Mean basal fluorescence (F_o) was assigned to each cell by averaging fluorescence intensity over the first 30 s (before tastant application). The $\Delta F/F$ fluorescence change during tastant stimulation was calculated as $[F_t - F_o] / F_o$ and the standard deviation of the pre-stimulus baseline determined (σo). Neurons were considered responders when $\Delta F/F$ exceeded 3.5 σ_o above F_o for at least two consecutive frames during the 10 s stimulation period (i.e. during the 10 s of tastant application); data were also analyzed using the significantly less stringent criteria of 2.5 and 3.0 standard deviations (see Fig. S7). All routines were built on a GUI software platform in Matlab to provide an interface that allows

visualization and manual editing at each step and permits analysis of experiments in minutes. Program is available upon request (Mariano Gabitto <mig2118@columbia.edu>)

Fig. S1 OGB1-AM labeled neurons in insular cortex

(a) Neurons were loaded with the calcium indicator OGB1-AM as described in Methods. (b) Labeled cells were identified and segmented using a semi-automated fast normalized cross-correlation routine (program available from Mariano Gabitto <mig2118@columbia.edu>). (c) To demonstrate that most neurons picked up the calcium indicator dye, the tissue was independently labeled with the cell impermeant dye Alexa-594 (*S10*). Panel (d) shows the super-imposition of panels (a) and (c); note that most cells were labeled with OGB1-AM; scale bar = 100 μm.

Fig. S2 Montage of imaging fields around the bitter hot spot

Vascular landmarks allow the registering of imaging fields in insular cortex. (a) Shown are 3 fields illustrating the clustering of the bitter-only responsive cells in the bitter hot spot; note the differences between the hot spot (field #3) and the adjacent fields (#1 and 2). (b) Also shown is a 700 x 350 μm field illustrating the sharp boundaries between a hot spot and surrounding cells. Scale bars: panel a = 300 μm, panel b = 100 μm.

Fig. S3 Different bitters are represented in the same cortical field, and activate a similar ensemble of neurons

(a) Responses in the bitter cortical field to 3 separate trials of 10 mM denatonium in the same animal. The rightmost panel and histogram illustrate the number of cells that responded to only 1 trial (white), those that responded to 2 of the trials (yellow) and those that responded to all three trials (red). Note the similarity in the patterns; at least 70% of the neurons responded to 2 of the 3 trials. Also shown are ΔF/F changes for 15 representative neurons (5 for each group) with each trial illustrated by a different color.

(b) Responses in the bitter cortical field to 3 separate bitters in the same animal (10 mM quinine, 1 mM cycloheximide, 10 mM denatonium). Upper panels illustrate single trials per bitter tastant. The rightmost panel and histogram illustrate the number of cells that responded to only 1 bitter (white), those that responded to 2 of the tastants (yellow) and those that responded to all three (red); ΔF/F traces are also shown for 5 representative neurons from each group, with each tastant illustrated by a different color. At least 70% of the neurons responded to 2 of the 3 tastants. Note

that the variability in trial-to-trial responses to a single bitter (panel a) are similar to the variability seen in trial-to-trial to different bitters (panel b).
(c) Responses as in panel (b), but now each panel shows the cells that responded at least twice to the single bitter tastants and their overlap. Scale bar = 50 μm.

Fig. S4 Single unit recordings from the bitter hot spot

To independently validate the segregation of single taste qualities into topographic cortical fields, we also performed single unit recording within (n=4 mice) and outside (n=9 mice) the bitter hot spot. The brain was exposed by surgical craneotony (see Methods), and the responses of cortical neurons inside and outside the hot spot were recorded using standard tungsten electrodes.

(a-b) Just as shown in the 2-photon imaging studies (Fig. 2), responding neurons within the bitter hot spot (demarked by the white dashes, panel a) preferred bitter versus any other taste quality (solid red circles); approximately 30 - 40% of the neurons in the hot spot (solid red versus open circles) displayed responses to taste stimuli, and these were tuned to bitter (panel b; n=13). In contrast, of the 39 neurons sampled outside the hot spot, 38 (indicated by the solid black circles) exhibited no statistically significant responses to taste stimuli, and only one (green) showed significant taste responses (to sweet stimuli) above basal spike frequency (one-way ANOVA $P < 0.05$). The relative location of all recorded neurons was determined by triagulating the position of the tungsten electrode to the MCA and RV landmarks (Scale bar = 0.5 mm).

(c) Shown are sample raster plots and peristimulus time histograms (PSTHs) to bitter stimuli from 2 neurons inside and 2 neurons outside the bitter hot spot; the box indicates the time and duration of the stimulus; the PSTHs used a bin of 500 ms. Shown to the right are the summary histograms (n=6 trials) in response to bitter (5 mM quinine), sweet (30 mM acesulfameK), umami (50 mM MPG + 1mM IMP), sour (10mM citric acid) and salt (100 mM NaCl).

Fig. S5 Selective responses from neurons in the sweet, umami and sodium-sensing receptive fields.

(a) In the sweet hot spot, sweet responsive neurons are highly tuned to sweet (green) versus other tastants. The graph shows the average peak $\Delta F/F$ (rank ordered) of 50 sweet responsive neurons

to a wide range of tastants; note the high selectivity for sweet stimuli. (b) Umami responsive neurons are tightly tuned to respond to umami stimuli (yellow). (c) Sodium-sensing neurons exhibit marked selectivity for NaCl (orange) over other tastants. Sweet = 30 mM acesulfameK, Umami = 100 mM MPG + 1mM IMP, NaCl = 100 mM NaCl, Bitter = 10 mM quinine, NaCl+amil = 100 mM NaCl + 10 μM amiloride and Sour = 10 mM citric acid. (d-f) Representative OGB-AM fluorescence changes from different neurons in the (d) sweet, (e) umami and (f) salt hot spots during sweet (green), bitter (red), sour (blue) and NaCl (orange) stimulation. Error bars are mean peak $\Delta F/F$ change ± s.e.m from ≥ 4 trials.

Fig. S6 Non-selective responses in the primary taste cortex.

(a) Typically, we can detect sparse patterns of activity in randomly distributed neurons of the insula, with no apparent spatial organization or correlated activity. This activity is seen independent of the nature of the taste stimuli (over most of the insula outside the hot-spots) and is not reproducible between trials (the 3 panels for each tastant represent 3 different trials; note that different subsets of cells are active in each trial). Similar results are also obtained with control tasteless artificial saliva (AS). (b) Histogram data, n = 14. Similar patterns of activity are observed in the primary taste cortex of mice lacking specific taste receptor function. Hence, this type of neural firing cannot represent a taste as it remains in mice that cannot taste. (c) Mice lacking sweet taste receptor function (T1R2-KO) still exhibit equivalent levels of neural firing when exposed to sweet (acesulfameK, 30 mM) or bitter (cycloheximide, 1mM) tastants; mean ± s.e.m, n = 3 animals. (d) T2R5-KO mice lacking the bitter receptor for cycloheximide still exhibit the same patterns of sparse, random activity when exposed to cycloheximide (1 mM) or to other bitter tastants (e.g. 10 mM quinine; n = 5 animals); scale bars = 100 μm.

Fig. S7 The basic tastes are represented by neurons selective for their preferred taste quality

Neurons in the bitter (a) and sweet (b) hot spots responded selectively to their preferred but not to other taste stimuli (see methods for details) (n = 4). Data were analyzed as described in methods, but responders were identified using 3 different threshold criteria: 2.5, 3.0 or 3.5 standard deviations above baseline. Although there were small differences in the number of

"responding cells" between conditions (compare bars), no differences in their organization into gustotopic clusters, or tastant selectivity were observed.

Fig. S8 Cells within a hot spot are not organized according to their response magnitude
(a) Neurons in the bitter hot spot were color-coded according to their response amplitude. Dark blue: ΔF/F 10-27.5%, Pale blue: ΔF/F 27.5-45%, yellow: ΔF/F 45-62.5%, red: ΔF/F 62.5-80%. Note the lack of any microstructure in their organization; similar results were obtained in multiple animals (n = 4). (b) Neurons in the sweet hot spot were also color-coded according to their response amplitude. Dark blue: ΔF/F 10-22.5%, Pale blue: ΔF/F 22.5-35%, yellow: ΔF/F 35-47.5%, red: ΔF/F 47.5-60%. Note the lack of any microstructure in their organization; similar results were obtained in multiple animals (n = 3).

References

S1. G. Q. Zhao *et al.*, *Cell* 115, 255 (Oct 31, 2003).

S2. K. L. Mueller *et al.*, *Nature* 434, 225 (Mar 10, 2005).

S3. G. Paxinos, K. B. J. Franklin, *The mouse brain in stereotaxic coordinates* (Academic Press, ed. 3rd Edition, 2007).

S4. G. Nelson *et al.*, *Nature* 416, 199 (Mar 14, 2002).

S5. C. N. Cearley *et al.*, *Mol Ther* 16, 1710 (Oct, 2008).

S6. K. Ohki, S. Chung, Y. H. Ch'ng, P. Kara, R. C. Reid, *Nature* 433, 597 (Feb 10, 2005).

S7. D. D. Stettler, R. Axel, *Neuron* 63, 854 (Sep 24, 2009).

S8. C. Stosiek, O. Garaschuk, K. Holthoff, A. Konnerth, *Proc Natl Acad Sci U S A* 100, 7319 (Jun 10, 2003).

S9. T. Komiyama *et al.*, *Nature* 464, 1182 (Apr 22, 2010).

S10. T. R. Sato, N. W. Gray, Z. F. Mainen, K. Svoboda, *PLoS Biol* 5, e189 (Jul, 2007).

Fig. S1

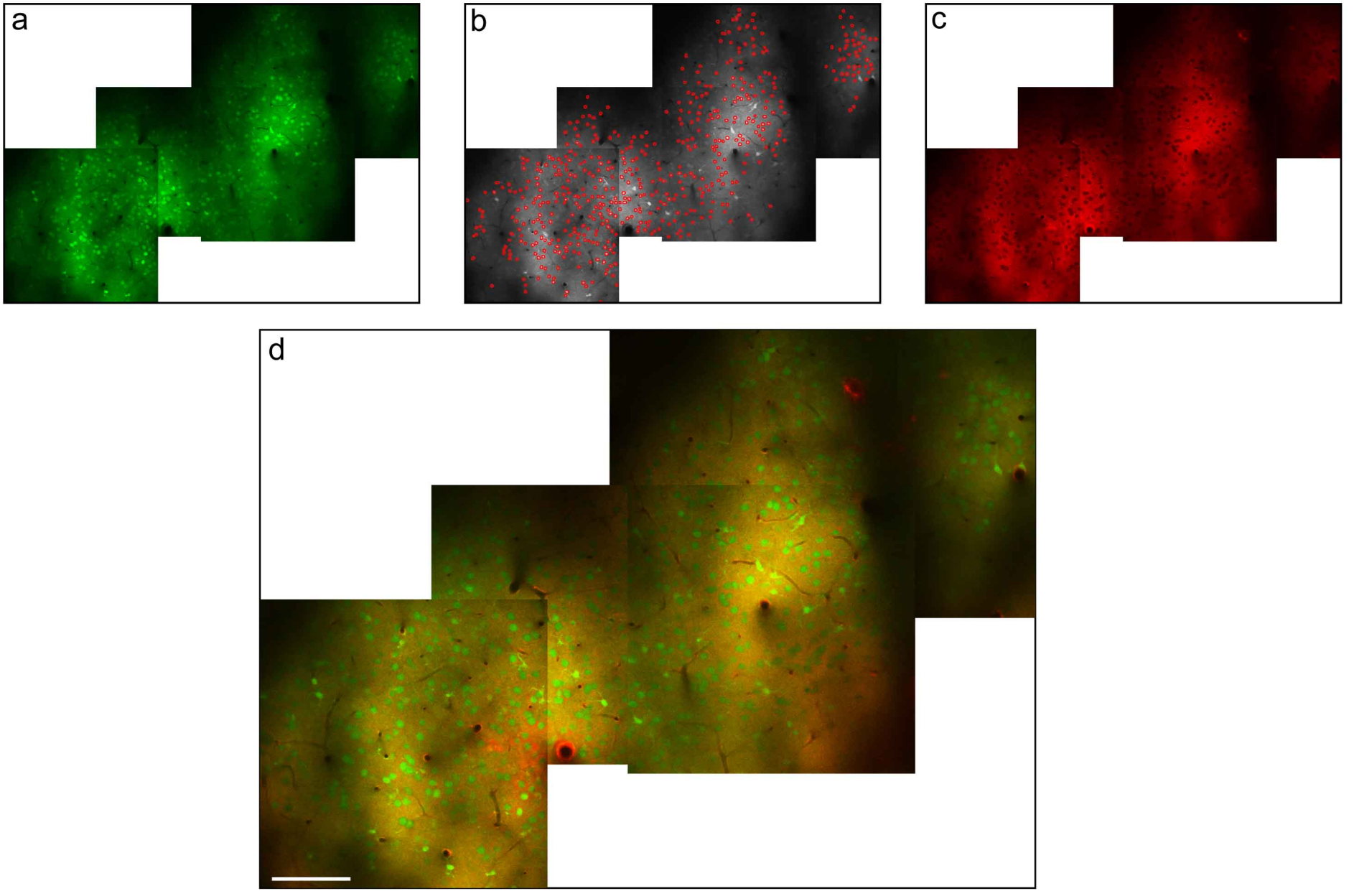

Fig. S2

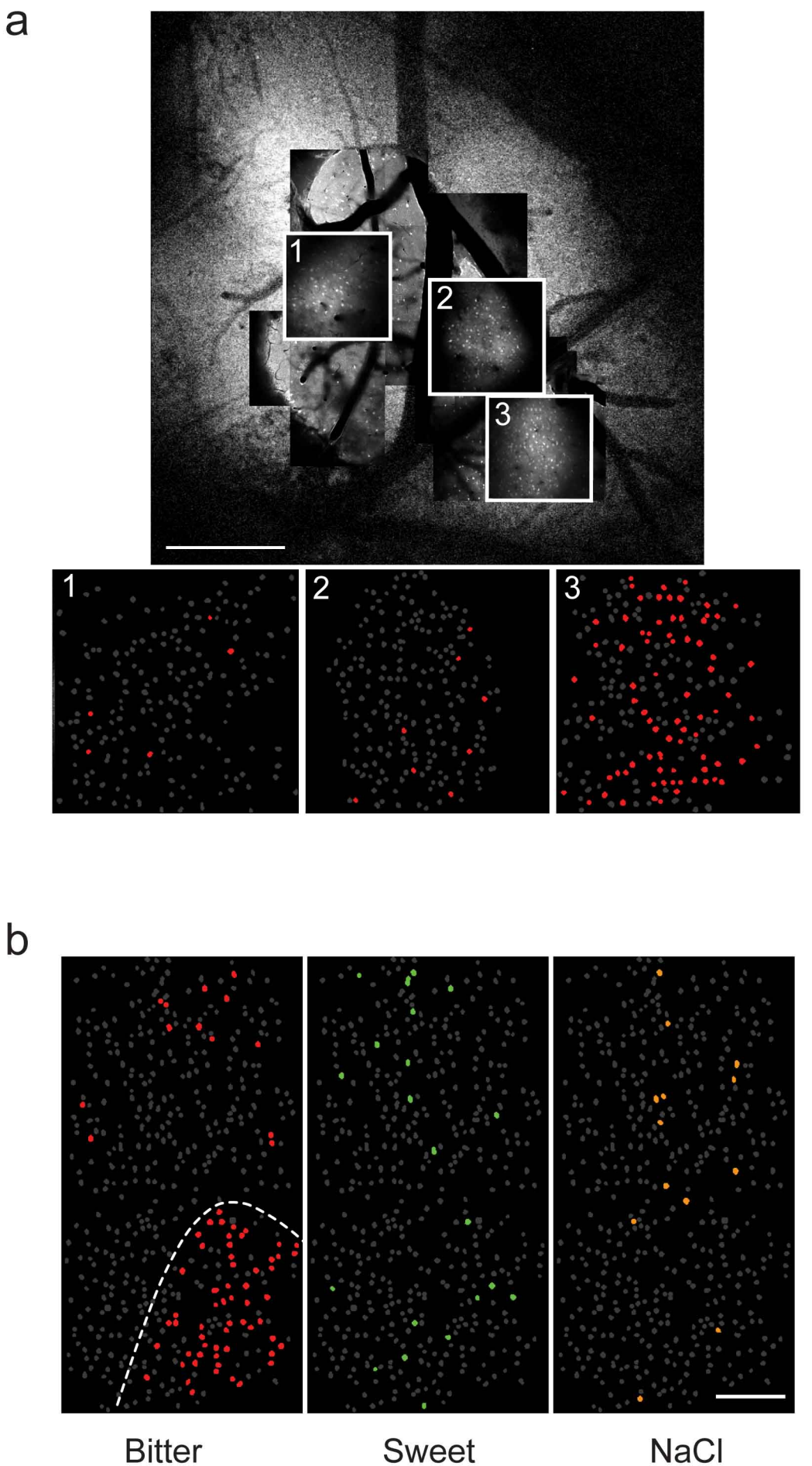

Fig. S3

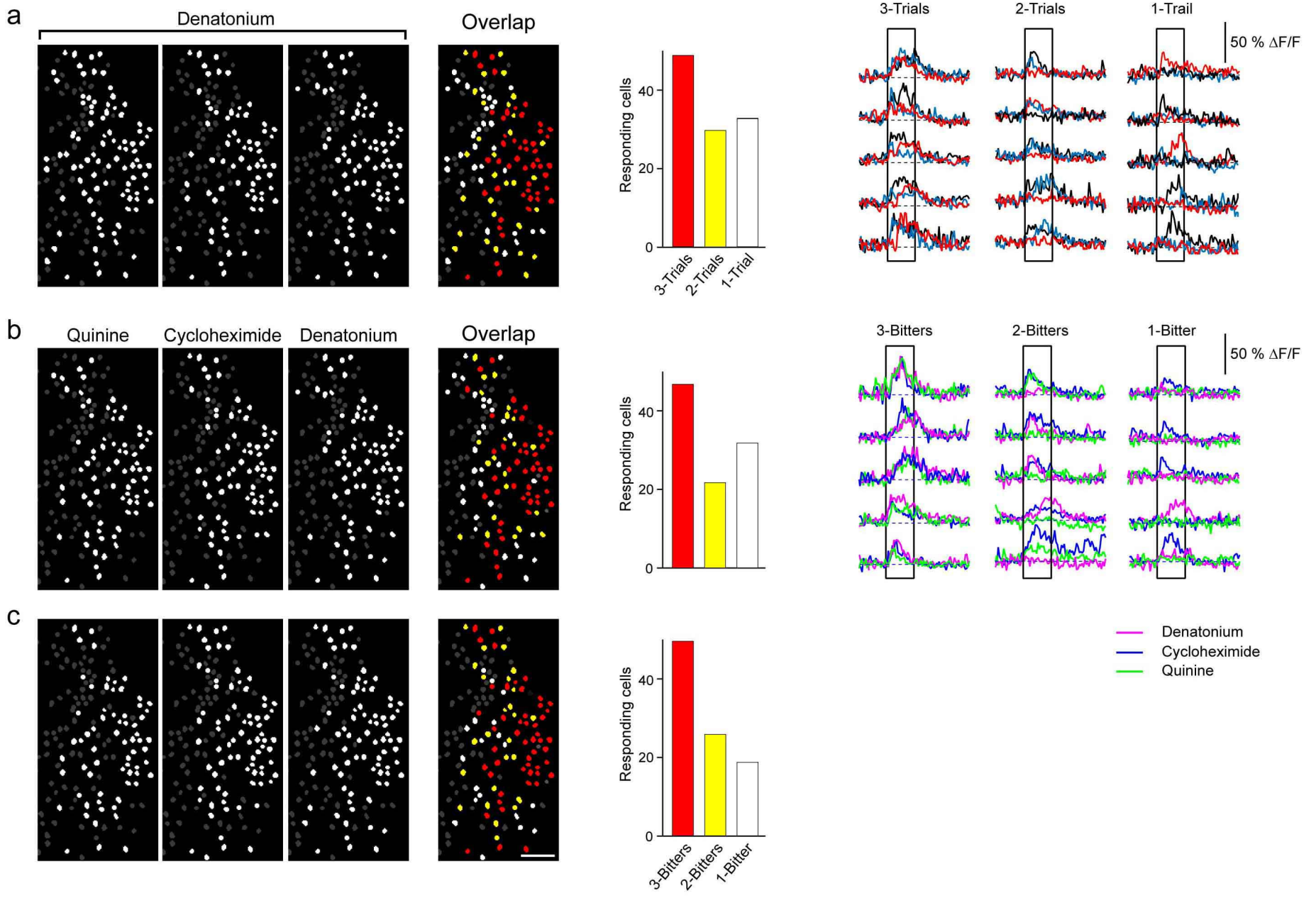
a
Denatonium
Overlap
Responding cells
40
20
0
3-Trials
2-Trials
1-Trial
3-Trials
2-Trials
1-Trail
50 % ΔF/F
b
Quinine
Cycloheximide
Denatonium
Overlap
Responding cells
40
20
0
3-Bitters
2-Bitters
1-Bitter
50 % ΔF/F
Denatonium
Cycloheximide
Quinine
c
Responding cells
40
20
0
3-Bitters
2-Bitters
1-Bitter

Fig. S4

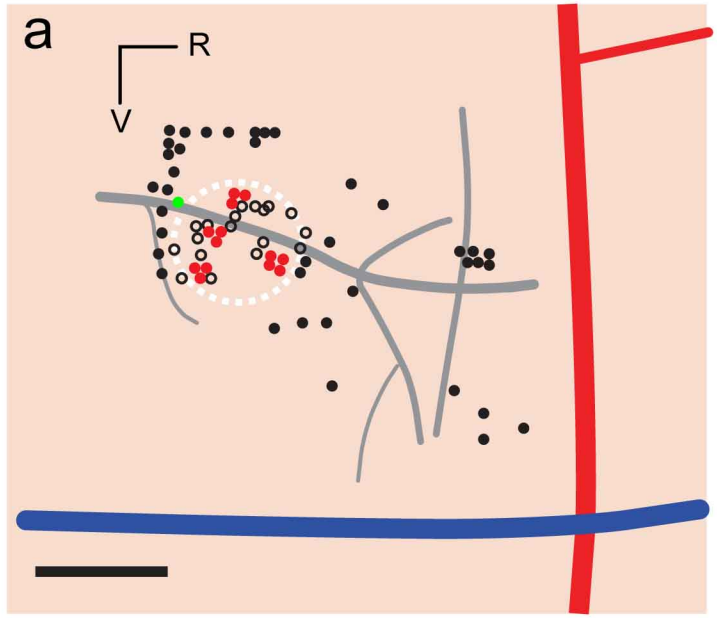
a
R
V

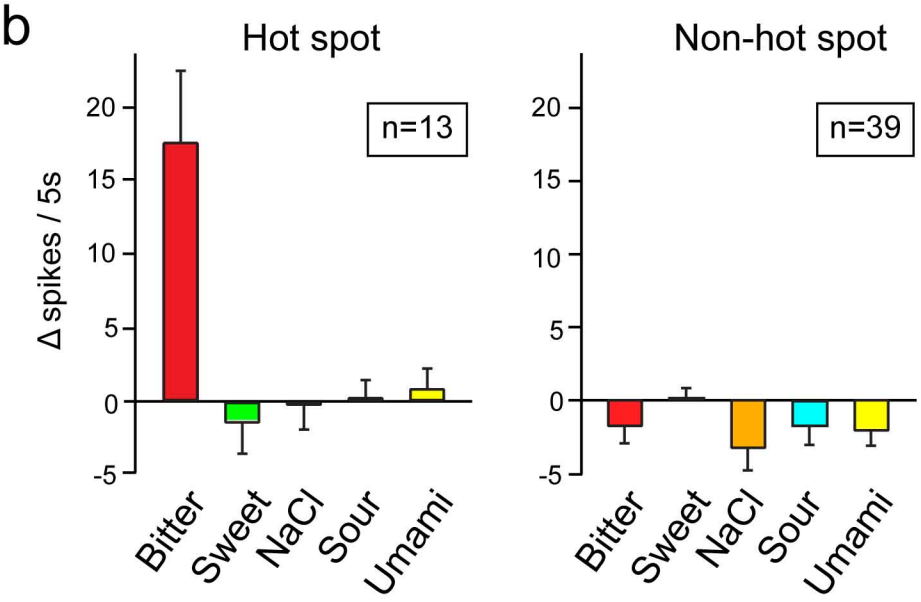
b
Hot spot
Non-hot spot
n=13
n=39
Δ spikes / 5s
Bitter
Sweet
NaCl
Sour
Umami

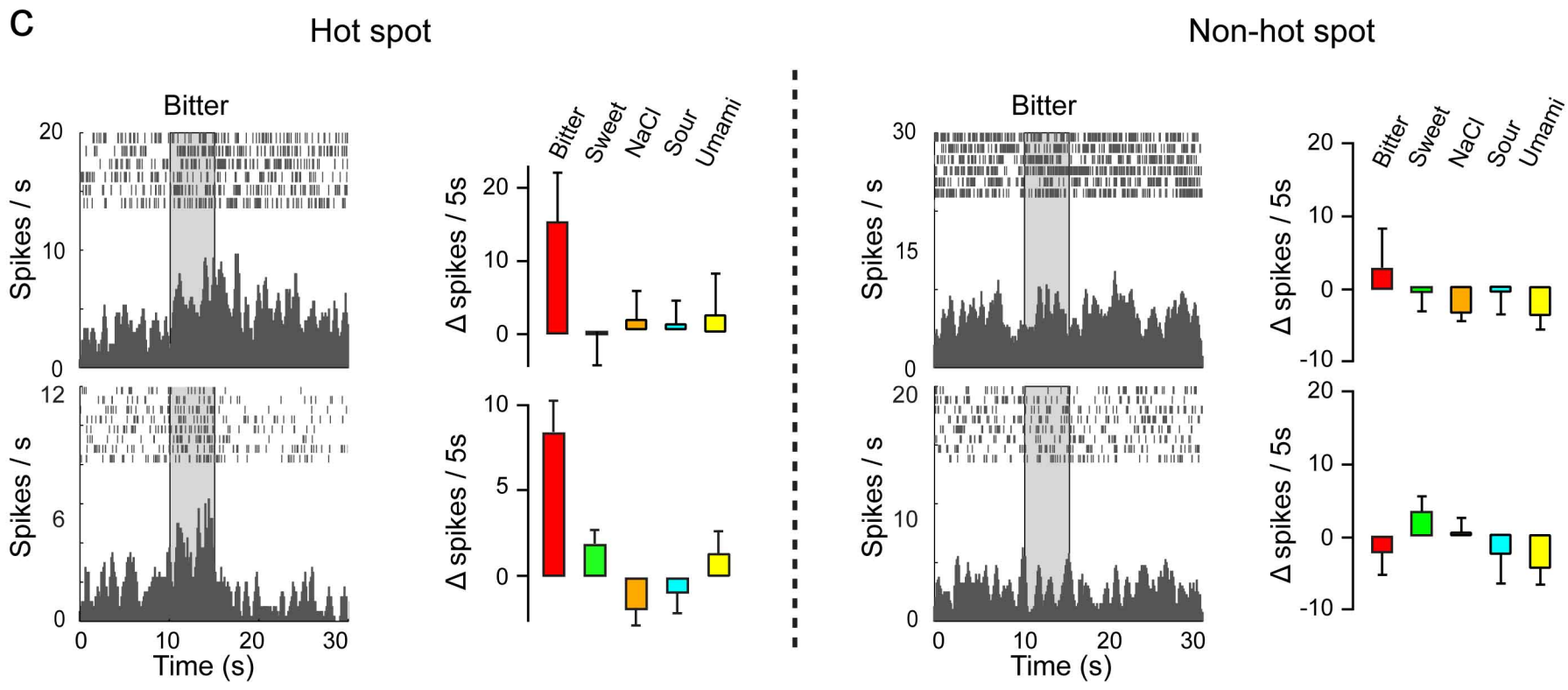
c
Hot spot
Non-hot spot
Bitter
Spikes / s
Time (s)
Δ spikes / 5s
Bitter
Sweet
NaCl
Sour
Umami

Fig. S5

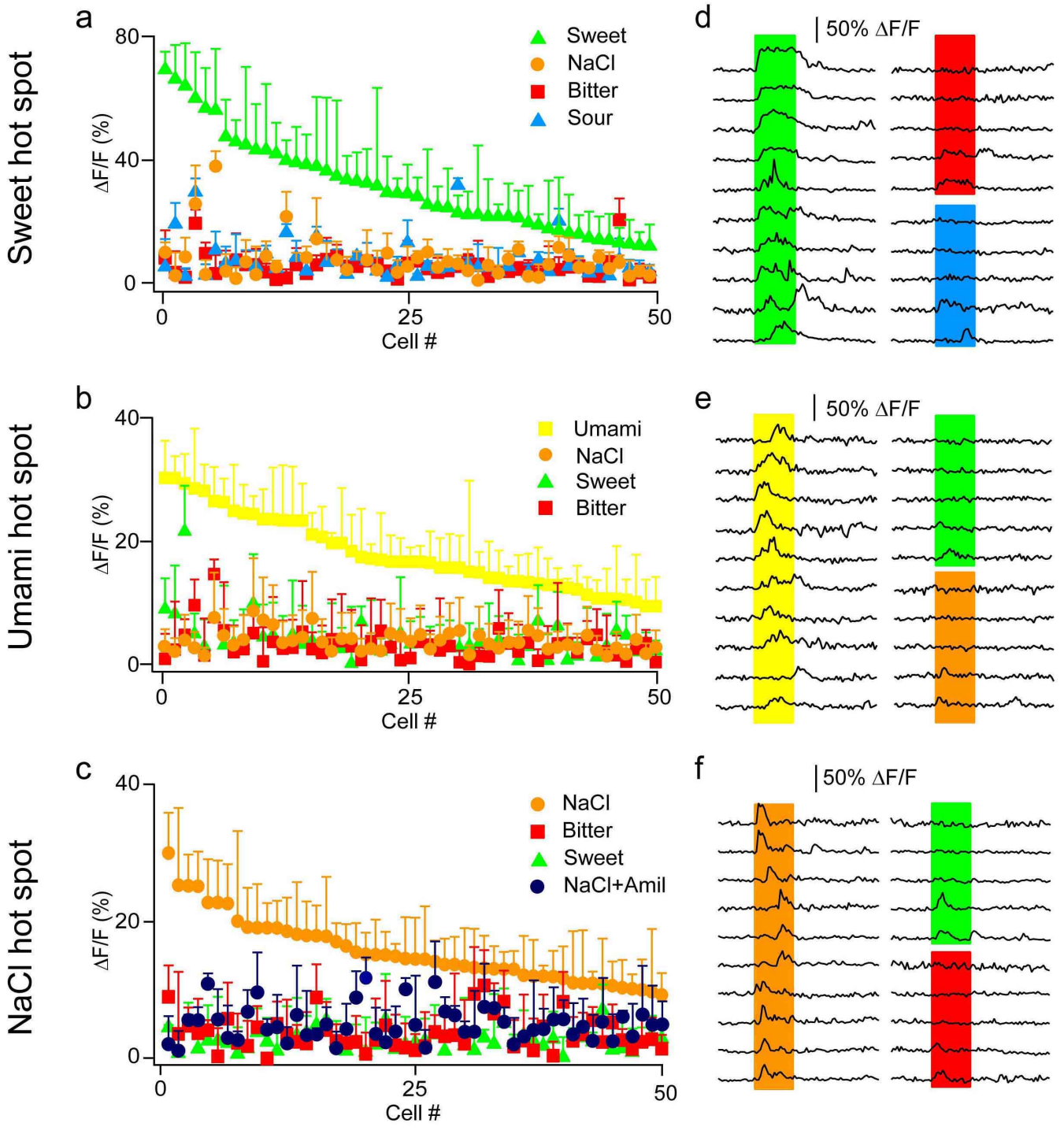
Sweet hot spot
a
80
40
0
ΔF/F (%)
0
25
50
Cell #
Sweet
NaCl
Bitter
Sour
d
50% ΔF/F
Umami hot spot
b
40
20
0
ΔF/F (%)
0
25
50
Cell #
Umami
NaCl
Sweet
Bitter
e
50% ΔF/F
NaCl hot spot
c
40
20
0
ΔF/F (%)
0
25
50
Cell #
NaCl
Bitter
Sweet
NaCl+Amil
f
50% ΔF/F

Fig. S6

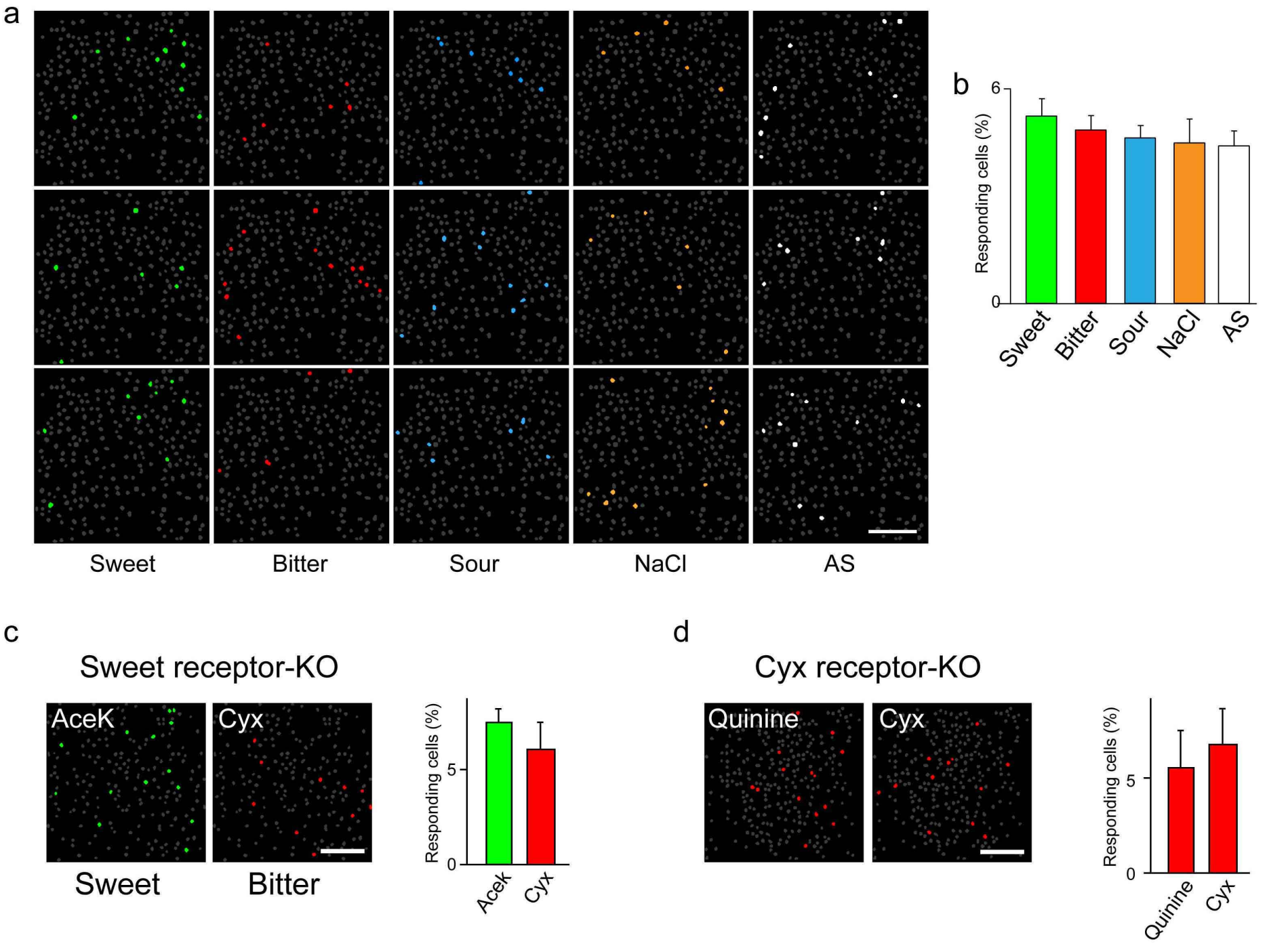
a
Sweet
Bitter
Sour
NaCl
AS
b
Responding cells (%)
6
0
Sweet
Bitter
Sour
NaCl
AS
c
Sweet receptor-KO
AceK
Cyx
Sweet
Bitter
Responding cells (%)
5
0
Acek
Cyx
d
Cyx receptor-KO
Quinine
Cyx
Responding cells (%)
5
0
Quinine
Cyx

Fig. S7

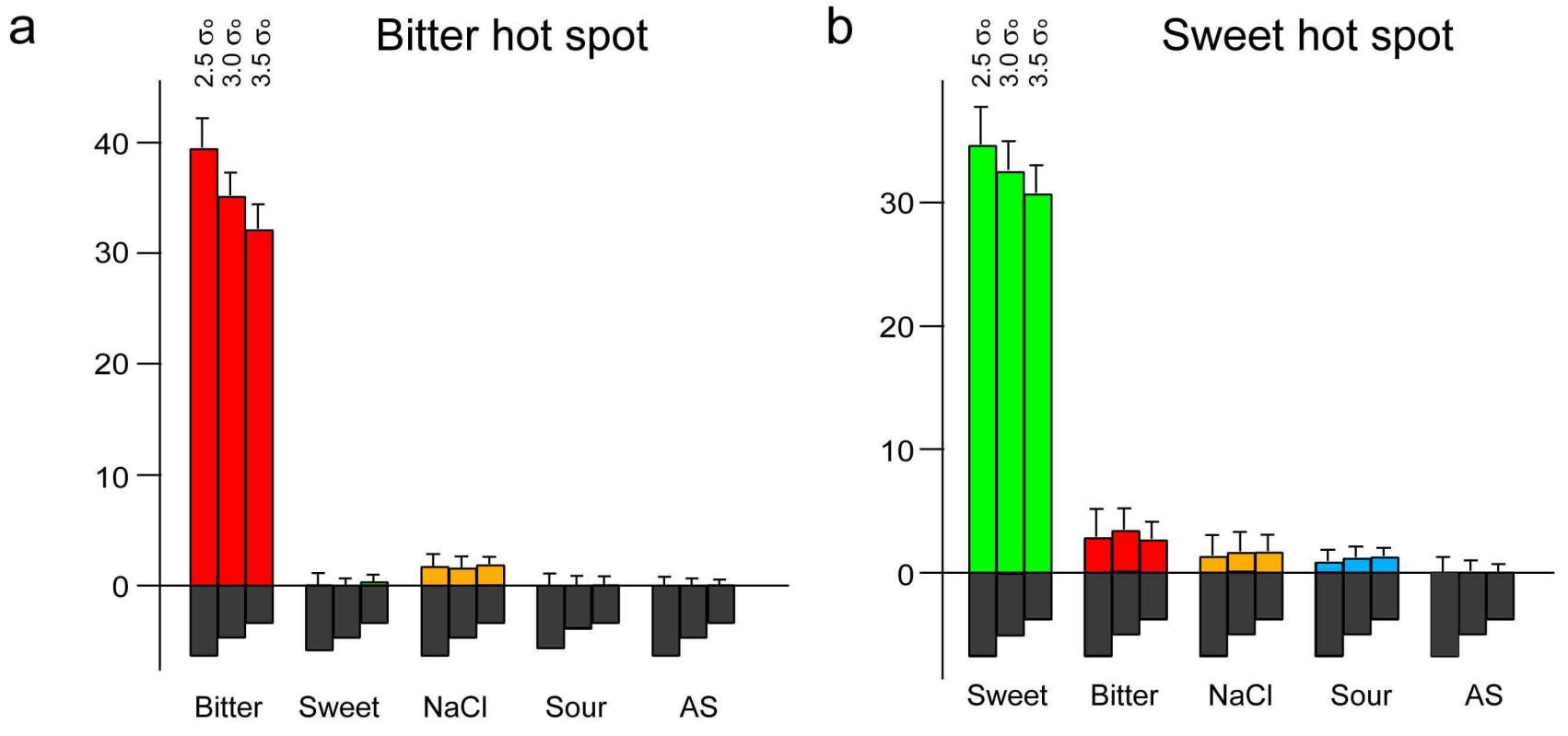
a
Bitter hot spot
2.5 σ₀
3.0 σ₀
3.5 σ₀
40
30
20
10
0
Bitter
Sweet
NaCl
Sour
AS
b
Sweet hot spot
2.5 σ₀
3.0 σ₀
3.5 σ₀
30
20
10
0
Sweet
Bitter
NaCl
Sour
AS

Fig. S8

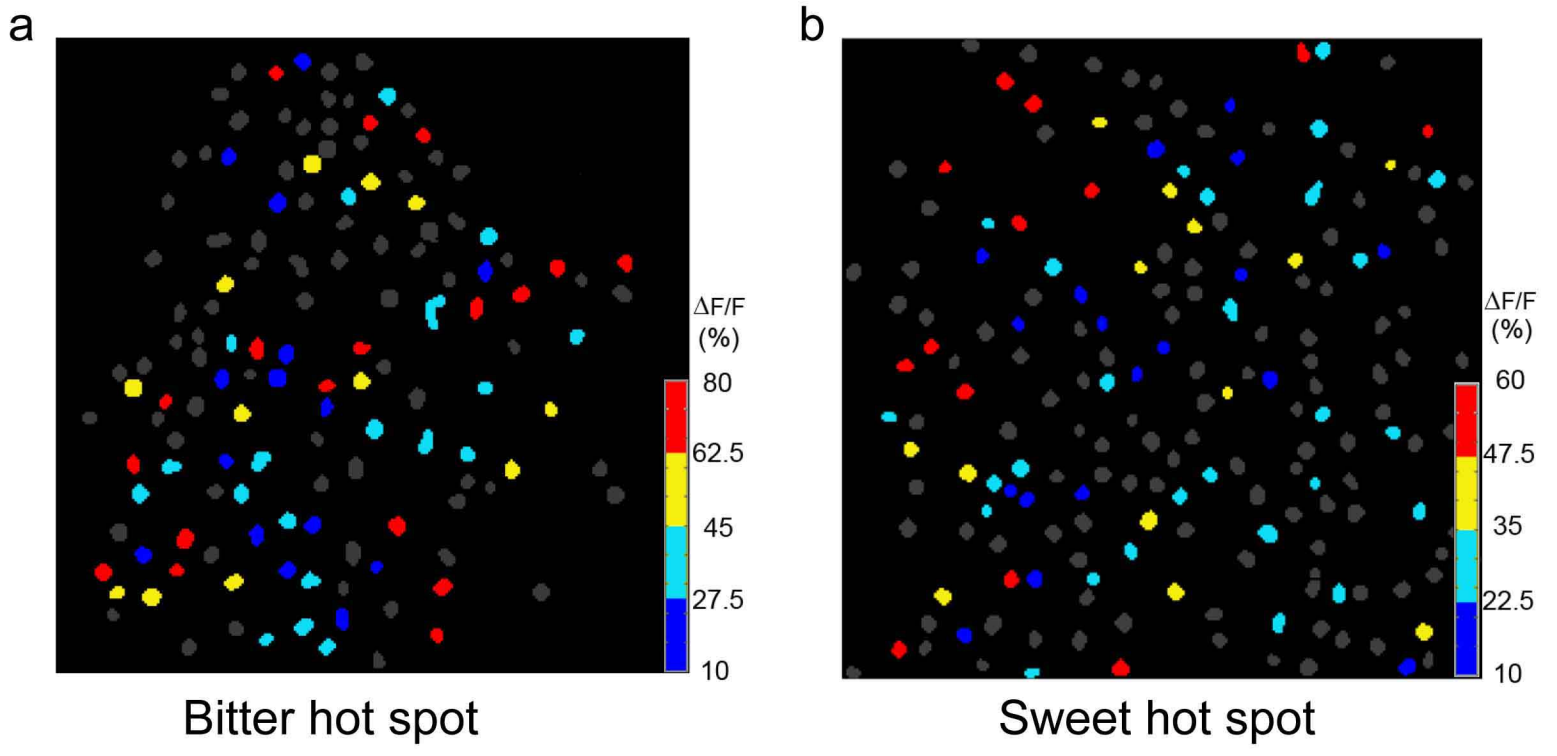
a
ΔF/F
(%)
80
62.5
45
27.5
10
Bitter hot spot
b
ΔF/F
(%)
60
47.5
35
22.5
10
Sweet hot spot